



Introduction to the quartz tuning fork

J.-M. Friedt, E. Carry

► To cite this version:

J.-M. Friedt, E. Carry. Introduction to the quartz tuning fork. American Journal of Physics, American Association of Physics Teachers, 2007, 75 (5), pp.415-422. 10.1119/1.2711826 . hal-00493935

HAL Id: hal-00493935

<https://hal.archives-ouvertes.fr/hal-00493935>

Submitted on 17 May 2021

HAL is a multi-disciplinary open access archive for the deposit and dissemination of scientific research documents, whether they are published or not. The documents may come from teaching and research institutions in France or abroad, or from public or private research centers.

L'archive ouverte pluridisciplinaire **HAL**, est destinée au dépôt et à la diffusion de documents scientifiques de niveau recherche, publiés ou non, émanant des établissements d'enseignement et de recherche français ou étrangers, des laboratoires publics ou privés.



Distributed under a Creative Commons Attribution| 4.0 International License

Introduction to the quartz tuning fork

J.-M. Friedt^{a)} and É. Carry^{b)}

Association Projet Aurore, UFR-ST La Bouloie, 16 route de Gray, Besançon, Besançon, France

We discuss various aspects of the quartz tuning fork, ranging from its original purpose as a high quality factor resonator for use as a stable frequency reference, to more exotic applications in sensing and scanning probe microscopy. We show experimentally how to tune the quality factor by injecting energy in phase with the current at resonance (quality factor increase) or out of phase (quality factor decrease), hence tuning the sensitivity and the response time of the probe to external disturbances. The principle of shear force scanning probe microscopy is demonstrated on a simple profiler constructed with equipment available in a teaching laboratory.

I. INTRODUCTION

Due to its high stability, precision, and low power consumption, the quartz crystal tuning fork has become a valuable basic component for frequency measurements. For instance, since the late 1960s, mechanical pendulum or spring-based watches have largely been replaced by crystal watches, which are sufficiently stable for most daily uses. The key component of these watches is mass produced at very low cost.

We will discuss the quartz tuning fork, a tiny component that includes a high quality factor resonator, which is used in a wide range of applications. A good understanding of its working principles will enable us to understand many applications to oscillators and sensors. We will describe the unique properties of the components provided by the piezoelectric substrates used for converting an electrical signal to mechanical motion and the resulting equivalent electrical Butterworth–Van Dyke circuit commonly used for modeling the behavior of the resonator.

The quality factor is a fundamental quantity for characterizing the behavior of the resonator under the influence of external perturbing forces. It is defined as the ratio of the energy stored in the resonator to the energy loss during each oscillation period. We will show how the interpretation of the quality factor depends on the measurement technique and how an external active circuit can be used to tune the quality factor. Finally, we will demonstrate the use of the tuning fork as a force sensor and use it in a simple demonstration of scanning probe microscopy.

II. THE RESONATOR

The basic principle of the tuning fork^{2–4} is well known to musicians: two prongs connected at one end make a resonator whose resonance frequency is defined by the properties of the material from which it is made and by its geometry. Although each prong can be individually considered as a first approximation to analytically determine the available resonance frequencies, the symmetry of the two prongs in a tuning fork reduces the number of possible modes with a good quality factor.^{3,5}

Using a piezoelectric substrate allows the mechanical excitation of the tuning fork (for example, hitting the tuning fork against a hard material) to be replaced by an electrical excitation. Piezoelectricity defines the ability of a material to convert a voltage to a mechanical displacement, and con-

versely, to generate electrical charges by the deformation of the crystalline matrix (assuming the appropriate symmetry conditions of the crystalline lattice are satisfied).

The stiffness of quartz provides an efficient means of confining the acoustic energy in the prongs of the tuning fork, so that we can reach large quality factors of tens of thousands at a fundamental frequency of 32 768 Hz under vacuum conditions. Combined with its tiny dimensions and low power consumption, these properties have made the quartz tuning fork the most commonly used electronic component when a stable frequency reference is required (such as clocks, digital electronics, and synchronization for asynchronous communications).

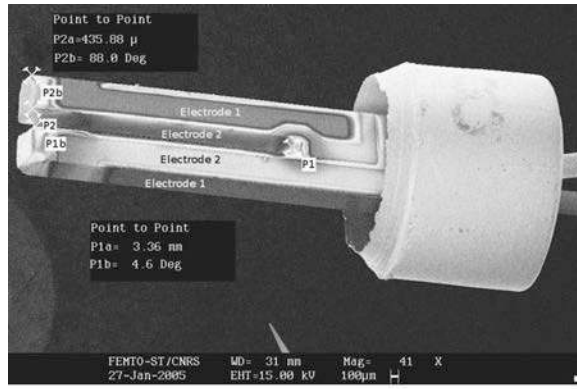
The tuning fork appears as a metallic cylinder 8 mm in height by 3 mm in diameter, holding a two-terminal electronic component. The packaging of the tuning fork can easily be opened by using tweezers to clamp the cylinder until the bottom of the cylinder breaks. A more reproducible way to open the packaging is to use a model-making saw to cut the metallic cylinder, keeping the bottom insulator as a holder to prevent the contact pins from breaking [Fig. 1(b)].

Figure 1(a) displays a scanning electron microscope image of the tuning fork and includes some of the most important dimensions used in the analytical model and in the finite element analysis to be discussed later in this document. This model was developed to study the influence of gluing a glass (optical fiber) or metallic tip to one of the prongs of the tuning fork as used in shear force scanning probe microscopy applications (Sec. IV B).

A preliminary analytical study of the tuning fork that does not require finite element analysis can be performed by assuming that each prong of the tuning fork behaves as a clamped beam: the frequency of the vibration modes of a single beam are obtained by including a free-motion condition on one boundary of the beam and a clamped condition on the other and solving for the propagation of a shear acoustic wave.^{6,7} The angular frequency ω_1 of the first resonance mode (for which there is no coupling between the two prongs) is then obtained numerically. The approximate solution is

$$\omega_1 = \frac{1.76a}{\ell^2} \sqrt{\frac{E}{\rho}}, \quad (1)$$

where $\ell \approx 3.2$ mm is the length of the prongs of the tuning fork, $a \approx 0.33$ mm their thickness, $E \approx 10^{11}$ N/m² the Young modulus of quartz, and $\rho = 2650$ kg/m³ its density.⁸ Equation



(a)



(b)

Fig. 1. (a) Scanning electron microscope image of a quartz tuning fork displaying the layout of the electrodes. (b) A tuning fork just removed from its packaging, and the metallic enclosure that would otherwise keep it under vacuum.

(1) gives a fundamental resonance frequency of approximately 32 kHz.

The position of the electrodes on the quartz substrate defines the way the deformation occurs when an electric field is applied, and hence the type of acoustic wave generated.⁹ For the common case of a quartz crystal microbalance, in which a quartz disk confines a bulk acoustic wave (as seen for example in high-frequency megahertz range quartz resonators such as those used with microcontrollers), the selected cut leads to a shear wave when an electric field is applied orthogonally to the surface of the quartz substrate, with the additional property of a negligible first-order resonance frequency shift vs temperature coefficient around 20 °C. For the tuning fork, electrodes of opposite polarities are deposited on adjacent sides of the prongs of the tuning fork, and the electric field thus generated induces a flexural motion of the prongs in the plane of the tuning fork (see Fig. 2). The tuning fork is etched using microelectronic clean room techniques in thin (a few hundred micrometers thick) Z-cut quartz wafers, that is, the normal to the wafer defines the *c*-axis of the quartz crystal, and the prongs of the tuning fork are oriented along the *Y*-axis.¹⁰ The electrodes are made of silver as shown by an energy dispersive x-ray (EDX) analysis (data not shown).

This selection of the orientation of the crystal and the way the electrodes are arranged on each beam defines the allowed vibration modes. The geometry of the prongs defines the resonance frequency. Several geometries can lead to a given frequency, usually 32 768 Hz. This frequency, which is equal to 2^{15} , makes it easy to generate a 1 Hz signal by a series of divide by two frequency dividers, as needed by the watch industry. The next closest possible oscillation mode is at 191 kHz, far enough from the fundamental mode to be easily filtered by the electronics.

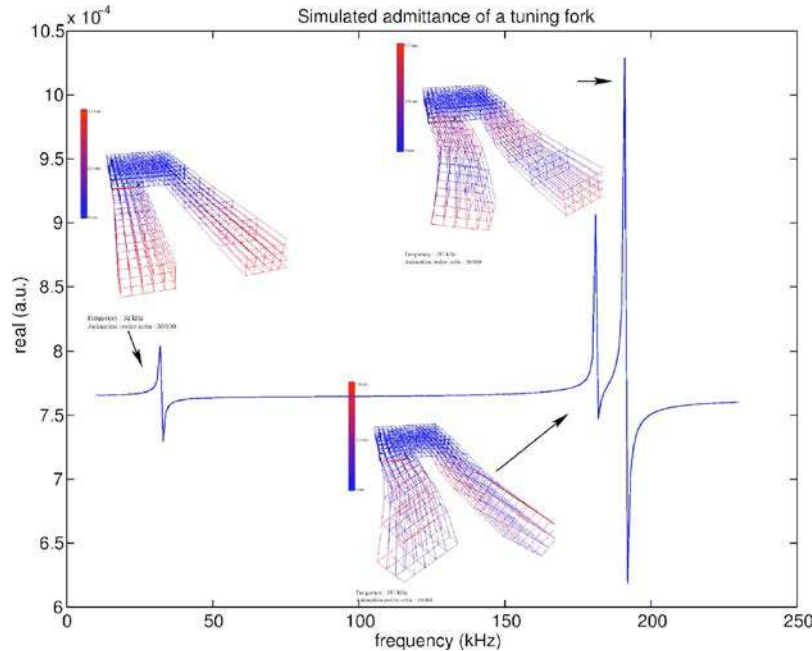


Fig. 2. Model of the motion at its first and third flexion resonance and first torsion modes of a tuning fork with quality factor $Q=1000$ under an applied potential of 0.5 V (simulation software developed by the team of S. Ballandras). All these modes were experimentally observed.

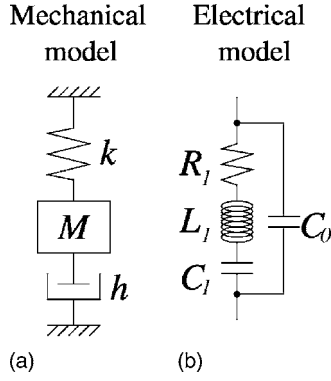


Fig. 3. (a) Mechanical model of the resonator as a damped oscillator and (b) electrical model which includes the motional (mechanical) equivalent series circuit in parallel with the electrical (capacitance between the electrodes separated by the quartz substrate) branch. See Table I for a summary of the equivalent quantities between the mechanical and electrical models.

III. USE IN AN OSCILLATOR

A. Mechanical and electrical models

All resonators can be modeled as a series resistance-inductor-capacitor circuit (RLC Butterworth–Van Dyke model)^{11,12} using an electrical analogy of a mechanical damped oscillator, in which the resistance represents the acoustic losses in the material and its environment, the inductor represents the mass of the resonator, and the capacitor represents the stiffness of the equivalent spring (see Fig. 3 and Table I). In addition to this mechanical branch, also called the motional branch, there is a purely electrical capacitance that includes the effect of the electrodes arranged along the piezoelectric substrate. Due to the low acoustic losses (small R) in piezoelectric materials, the resulting quality factor is usually on the order of tens of thousands. In air, the quality factor usually drops to a few thousand because of losses due to friction between the resonator and air. Quartz tuning forks are not appropriate for a liquid medium because the motion of the prongs generates longitudinal waves in the liquid, dissipating much of the energy stored in the resonator, and hence leading to a quality factor of order unity. Furthermore, because there is a potential difference between the electrodes, which are necessarily in contact with the liquid, there are electrochemical reactions when solutions have high ionic content.

Table I. Summary of the equivalent quantities between the mechanical and electrical models presented in Fig. 3. Typical values are $C_0 \approx 5$ pF and $C_1 \approx 0.01$ pF, yielding an inductance value L_1 in the kHz range and a motional resistance in the tens of k Ω range. The unique property of quartz resonators is such a huge equivalent inductance in a tiny volume.

Mechanical	Electrical
h (friction)	R_1 (resistance)
M (mass)	L_1 (inductor)
k (stiffness)	$1/C_1$ (capacitance)
x (displacement)	q (electrical charge)
\dot{x} (velocity)	$i = dq/dt$ (current)
$M\ddot{x} + h\dot{x} + kx = F$	$L_1\ddot{q} + R_1\dot{q} + q/C_1 = U$
$Q = 1/h\sqrt{kM}$	$Q = 1/R_1\sqrt{L_1/C_1}$ (quality factor)
$\omega_0 = \sqrt{k/M}$	$\omega_0 = 1/\sqrt{L_1C_1}$ (angular frequency)

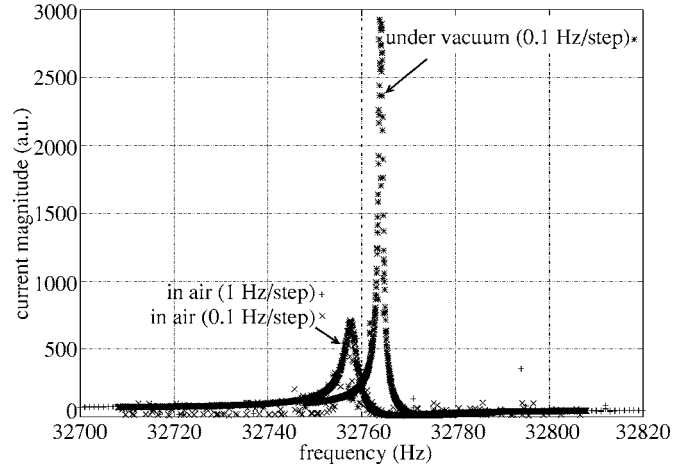


Fig. 4. Current measurement through packaged and opened tuning forks as a function of frequency. We observe first the resonance followed by the antiresonance. Notice the signal drop and the peak widening due to viscous friction with air once the tuning fork is removed from its packaging.

The electrical model of the tuning fork differs from the classical damped oscillator by the presence of a capacitor C_0 parallel to the RLC series components (see Fig. 3). The result of this parallel capacitance is an antiresonance at a frequency above the resonance frequency. At resonance, the resonator acts as a pure resistance, with maximum current since the magnitudes of the impedance of the capacitance and inductance in the motional branch are equal; the antiresonance is characterized by a minimum in the current at a frequency just above the resonance frequency. Both the resonance and antiresonance are clearly seen in the experimental transfer functions in which the current through the tuning fork vs frequency is measured (see Fig. 4).

B. Electrical characterization of the resonator

A resonator that is to be used as a sensor and whose characteristics are affected by the environment can be monitored in two ways: either in an oscillator where the resonator is included in a closed loop in which the gains exceed the losses (consistent with the Barkhausen phase conditions¹³), or in an open-loop configuration in which the phase behavior at a given frequency is monitored over time by an impedance analyzer. Because such a characterization instrument is expensive and usually not available in teaching labs, we have built an electronic circuit based on a digital signal synthesizer.

We have chosen to work only in an open-loop configuration (by measuring the impedance of the tuning fork powered by an external sine wave generator) rather than including the resonator in an oscillator loop. A 33 kHz stable oscillator circuit is easy to build, for instance, by means of a dedicated integrated circuit: the CMOS 4060.¹⁴ However, the phase changes in the tuning fork in sensor applications—of order of 10° —only yield small frequency changes of order of a fraction of a hertz at resonance, difficult to measure without a dedicated research grade frequency counter (such as Agilent 53132A). A resonator of quality factor Q at the resonance frequency f_0 will have a phase shift $\Delta\varphi$ with a frequency shift Δf given by $\Delta\varphi = -2Q\Delta f/f_0$.¹⁵ In our case, $f_0 \approx 32\,768$ Hz and $Q \approx 10^3$ (tuning fork in air, Fig. 4), so that a resonance frequency variation of 2 to 3 Hz is expected.

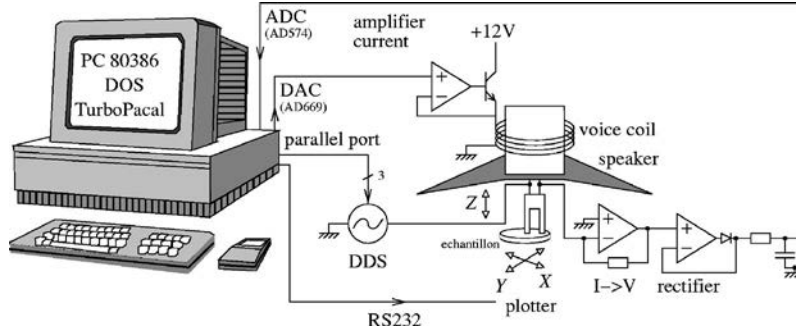


Fig. 5. Experimental setup, including the frequency synthesizer generating the signal for probing the tuning fork and the current to voltage converter, followed by the low-pass filter. Both elements are intended to condition the signal, which is then digitized for computing the feedback current generated by the digital to analog converter. This current, fed to the voice coil, is the quantity later plotted as a function of sample position for mapping the topography of the samples.

Although such a frequency variation is easily measured with dedicated equipment, care should be taken when designing an embedded frequency counter as will be required by the experiments described in Sec. IV B. Designing such a circuit is outside the scope of this article. We will thus describe a circuit that generates a sine wave with high stability to examine the vibration amplitude of the tuning fork.

A frequency synthesizer is a digital component that, from a stable clock (usually a high-frequency quartz-based oscillator) at frequency f_C , generates any frequency from 0 to $f_C/3$ by $f_C/2^{32}$ steps. An example is the Analog Devices AD9850 32 bits frequency counter (see Fig. 5). The sine wave is digitally computed and converted to an output voltage by a fast digital-to-analog converter. Such stability and accuracy are needed to study the quartz tuning fork whose modest resonance frequency (about 32 768 Hz) must be generated with great accuracy because of its high quality factor: a resolution and accuracy of 0.01 Hz will be needed for the characterizations of the tuning fork and the design of the scanning probe profiler as discussed in this paper (Fig. 4).

The frequency synthesizer excites the tuning fork. Its impedance drops at resonance and the current is measured by a current to voltage converter using an operational amplifier (TL084) that provides the virtual ground and avoids loading the resonator. The magnitude of the voltage at the output of the current-voltage converter is rectified and low-pass filtered with a cutoff frequency below 3 kHz [see Fig. 5(b)].

Figure 4 shows experimental results of resonators under vacuum (encapsulated) and in air after opening their packaging. In both cases, a current resonance (current maximum) followed by an antiresonance (current minimum) are seen, both of which are characteristic of a model including a series RLC branch (acoustic branch) in parallel with a capacitor (electrical branch). The resonance frequency and the maximum current magnitude both decrease when the tuning fork is in air, and the quality factor drops. Both effects are due to the viscous interaction of the vibrating prongs with air. Compressional wave generation in air dissipates energy, leading to a drop in the quality factor. The quality factor is about 10 000 in vacuum and about 1000 in air. The resonance frequency drops from 32 768 Hz in vacuum to 32 755 Hz in air.

IV. SENSOR ASPECTS

As in any case in which a stable signal that is insensitive to its environment can be obtained, we can ask how the geometry of the resonator might be disturbed to lead to a

sensitive sensor. One solution for the tuning fork is to attach a probe to one prong, which is sensitive to the quantity to be measured.

Applying a force to a probe disturbs the tuning fork's resonance frequency, which can be measured with great accuracy to yield a sensitive sensor. The probe can be a tip vibrating over a surface whose topography is imaged, leading to tapping mode microscopy,¹⁶ or a shear force scanning probe microscope.^{10,17} A topography measurement can be combined with the measurement of other physical quantities¹⁸ such as the electrostatic force,¹⁹ magnetic force,²⁰ or the evanescent optical field.^{21,22}

A. Force sensor

We have seen that due to the vibration of the prongs of the tuning fork with a displacement component orthogonal to the sides of the prongs, a fraction of the energy stored in the resonator is dissipated at each oscillation by interaction with the surrounding viscous medium, leading to a drop in the quality factor and a sensitivity loss. This result mostly excludes the use of the tuning fork as a mass sensor in a liquid medium because the viscous interaction would be too strong.

We have glued iron powder to the end of the prongs of the tuning fork to make a magnetometer.²³ The results of this experiment lacked reproducibility because the weight of the glue and iron is difficult to control. The effect of the magnetic force on the prongs depends on the amount of iron glued to the prongs, which should be controlled when glued. Also the magnetic force, which varies as the inverse cube of the distance, is a short-range force that is especially difficult to measure.

B. Profiler

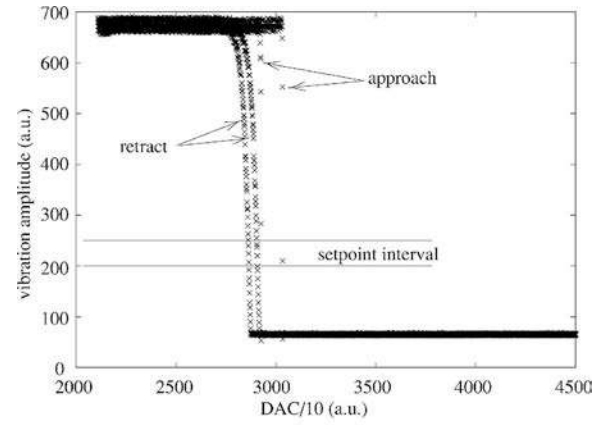
To illustrate the use of a tuning fork to monitor the probe to surface distance, we built a profiler: this design of this instrument illustrates the general principles of shear force microscopy. In this case the perturbation of the resonance frequency provides information on the surface due to close contact with the prong of the resonator. In practical examples, in which excellent spatial resolution is required, a tip is glued to the end of the tuning fork. Such a setup is too complex for our elementary discussion, and we will use one corner of the tuning fork as the probe in contact with the surface of interest.

Shear force microscopy provides a unique opportunity to decouple a physical quantity such as the tunneling current, the evanescent optical field, or the electrochemical potential, and the probe to surface distance. Many scanning probe techniques use the physical quantity of interest as the probe-surface distance indicator. Such a method is valid for homogeneous substrates in which the behavior of the physical quantity is known and is constant over the sample. For a heterogeneous sample, it is not known whether the observed signal variations are associated with a change of the probe-surface distance or with a change in the properties of the substrate. By having a vibrating probe attached to the end of a tuning fork, the physical quantity can be monitored while the feedback loop for keeping the probe-sample distance constant is associated with the tuning fork impedance. Such a decoupling should be more widely used than it is in most scanning probe techniques. As far as we know, near-field optical microscopy is the only method that takes great care to decouple the tip-sample distance and the measurement of the evanescent optical field.

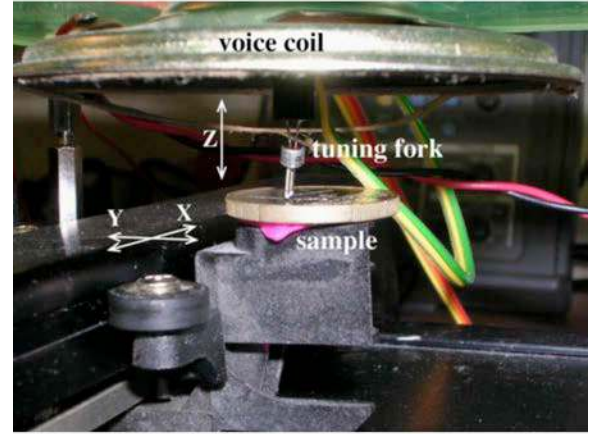
The experimental setup for keeping the probe-sample distance constant is very similar to that presented earlier in Ref. 24 with a fully different probe signal:

- (1) The tuning fork oscillates at its resonance frequency and always works at this fixed frequency.
- (2) The tuning fork is attached to an actuator, making it possible to vary its distance to the surface being analyzed (the Z direction): a 70 mm diameter, 8 Ω loud speaker (as found in older personal computers) is controlled using a current amplified transistor polarized by a digital to analog converter as shown in Fig. 5(b).
- (3) The relation between the current through the vibrating tuning fork and its distance to the surface is measured. We observe that it is bijective [each probe-sample distance yields a unique current value, Fig. 6(a)], but displays hysteresis. Bijectivity means that we can find a range in the probe-sample distance for which a unique measurement is obtained for a given distance, and this measurement is a unique representative of that distance.
- (4) The sample is attached to a computer-controlled (RS232) plotter to perform a raster scan of the surface and to measure automatically the probe-surface distance and thus reconstruct the topography of the sample (which, in our case, is a coin—see Fig. 7).

The basic principle of each measurement is as follows: for each new point, the vibration amplitude of the tuning fork is measured, and the current through the voice coil of the loud speaker is adjusted (using the D/A converter) until the tuning fork interacts with the surface and its vibration amplitude reaches the set-point value chosen in the region where the slope of the signal (current magnitude)-distance relation is greatest. The value of the D/A converter for which the set-point condition is met is recorded and the plotter moves the sample under the tuning fork to a different location. Feedback on the vibration magnitude²⁵ is less sensitive than feedback on the phase between the current through the tuning fork and the applied voltage, but this quantity is more difficult to measure and requires the tuning of an additional electronic circuit.²⁶ Two possible methods have been selected but have not been implemented here: either sending the saturated voltage and current signals through a XOR gate, whose output duty cycle is a function of the phase between the two



(a)



(b)

Fig. 6. (a) Magnitude of the current through the tuning fork as a function of the probe-surface distance. (b) Picture of the experimental setup. Only a corner of the tuning fork is in contact with the sample in order to achieve better spatial resolution.

input signals; or multiplying the two input signals (using an AD633) followed by a low-pass filter. Only the dc component proportional to the cosine of the phase is obtained, assuming that the amplitude of the two input signals is constant, which requires an automatic gain control on the current output of the tuning fork. The latter method is fully implemented in the Analog Devices AD8302 demodulator.

It can be seen in Fig. 6(b) that the tuning fork is tilted with respect to the normal of the coin surface and the motion of the prong is not parallel to the surface. Thus, the interaction of the prong of the tuning fork in contact with the surface is closer to that of a tapping mode atomic force microscope^{27,28} than to a true shear force microscope.

V. QUALITY FACTOR TUNING

A. The quality factor

The quality factor Q is widely used when discussing oscillators, because this property is useful for predicting the stability of the resulting frequency around the resonance following, for instance, the Leeson model which relates the phase fluctuations of the oscillator with the quality factor of the resonator and the noise properties of the amplifier used for running the oscillator.¹³ There are several definitions of

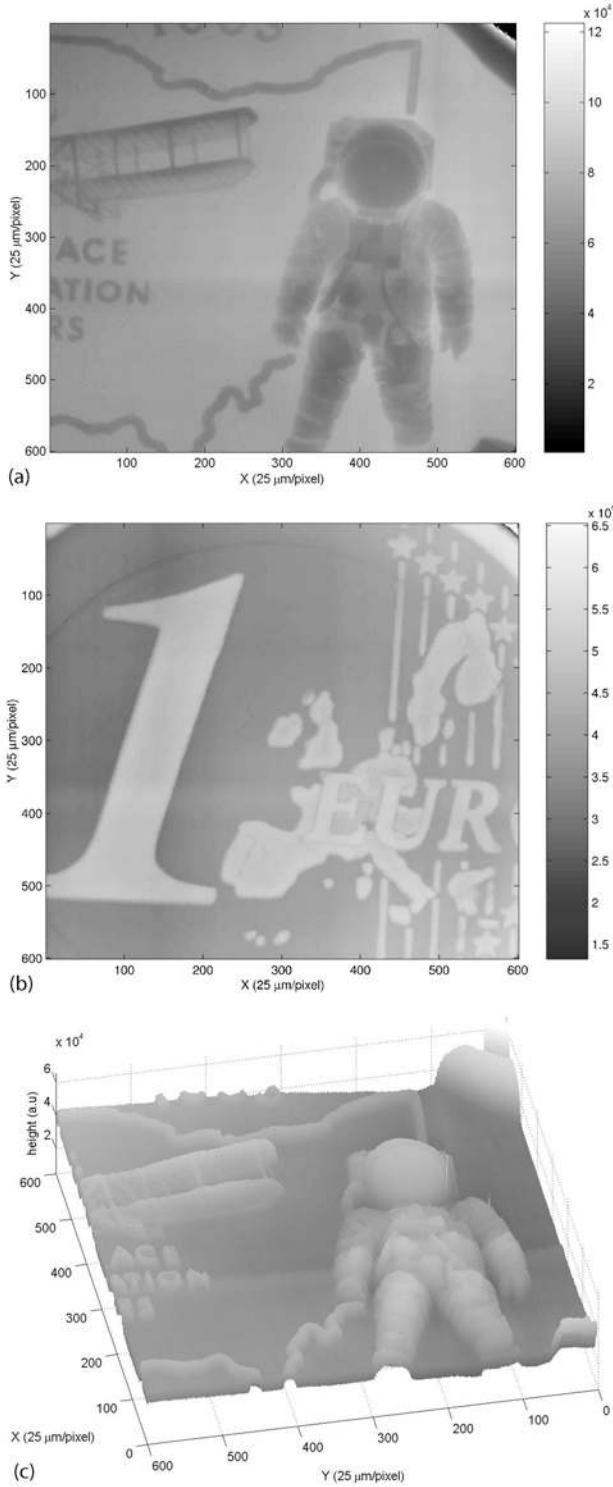


Fig. 7. (a) topography of a US quarter and (b) topography of a 1 Euro coin. (c) 3D representation of the topography of the quarter. All scans are 600×600 pixels with a step between each pixel of $25 \mu\text{m}$.

the quality factor including the following:

- (1) The ratio of the energy stored in the resonator to that dissipated during each period. This ratio is the fundamental definition of Q .
- (2) The width at half height of the power spectrum, or the width at $1/\sqrt{2}$ of the admittance plot. [Note that 20

$\times \log_{10}(\sqrt{2}) = 3$, and we look for the peak width at -3 dB of the maximum value in a logarithmic plot.]

- (3) When the excitation of the resonator at resonance stops, the oscillator decays to $1/e$ of the initial amplitude in Q/π periods.
- (4) The slope of the phase vs frequency at resonance is π/Q . This relation is associated with the phase rotation around the resonance during which the resonator behavior changes from capacitive to inductive, that is, a phase rotation of π over a frequency range of $\approx f_0/Q$ with f_0 equal to the resonance frequency.

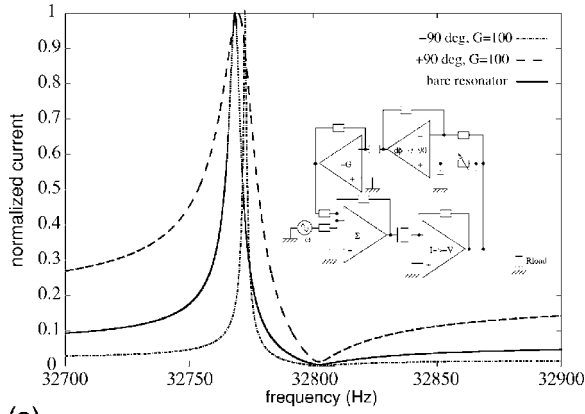
The first point of view based on energy is the fundamental definition of the quality factor to which all other assertions are related: the second and third definitions additionally assume that the resonator follows a second-order differential equation. Such an assumption is correct only if the quality factor is large enough ($Q > 10$), so that the resonator can always be locally associated with a damped oscillator. This assumption is always true for quartz resonators, for which the quality factor is observed to be in a range of hundreds to thousands. The mechanical analogy of the damped oscillator leads to the ratio of the quality factor to the angular frequency being equal to the ratio of the mass of the resonator to the damping factor, which can be associated with the ratio of the stored energy to the energy loss per oscillation period.

B. Tuning the quality factor

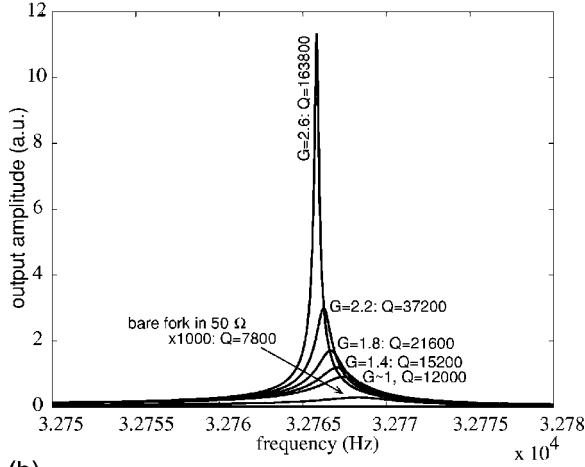
From the fundamental definition, we can infer that the quality factor can be increased by injecting energy into the tuning fork during each cycle. Similarly, the quality factor can be decreased by removing energy during each cycle. These two cases can be accomplished by adding a sine wave at the resonance frequency with the appropriate phase. The limit to enhancement of the quality factor is the case in which more energy is injected into the resonator than the amount that is lost: the resonator never stops vibrating and an oscillator loop has been achieved. In this case, the Barkhausen phase condition for reaching the oscillation condition is a particular case of quality factor enhancement, and the magnitude condition (the amplifier gain compensates for the losses in the resonator) is a special case of an infinite quality factor.

In practice, a quartz tuning fork works at a low enough frequency to allow classical operational amplifier based circuits to be used for illustrating each step of quality factor tuning. Figure 8(a) illustrates a possible implementation of the circuit including an amplifier, a phase shifter, a bandpass filter, and an adder, as well as the simulated Spice response of the circuit in which the Butterworth–Van Dyke model of the quartz tuning fork is replaced by the actual resonator. The feedback gain defines the amount of energy fed back to the resonator during each period; the phase shift determines whether this energy is injected in phase with the resonance (quality factor increase) or in phase opposition (quality factor decrease). The output is fed through a bandpass filter to ensure that only the intended mode is amplified and that a spurious mode of the tuning fork does not start oscillating. Eventually, the feedback energy added to the excitation signal closes the quality factor tuning loop.

Figure 9 displays a measurement of quality factor increase based on a discrete component implementation of the circuit in Fig. 8. The resonance frequency shift is associated with a



(a)



(b)

Fig. 8. (a) Circuit used for quality factor tuning and Spice simulation of the response as a function of amplifier gain. In addition to the quality factor enhancement, a frequency shift is associated with the phase of the feedback loop not being exactly equal to $\pm 90^\circ$. The normalized current is displayed for enhancing the visibility of the quality factor tuning. (b) Current output as a function of feedback loop gain leading to in-phase energy injection and current magnitude increase with the enhancement of the quality factor.

feedback loop phase that is not exactly equal to 90° . The phase shift was set manually, using a variable resistor and an oscilloscope in XY mode, until a circle was drawn by an excitation signal and by the phase-shifted signal, allowing for a small error in the setting.

VI. SUMMARY

We have discussed the quartz tuning fork, a two-terminal electronic component whose use is essential in applications requiring an accurate time reference. We have shown its basic principle when used as a high quality factor resonator packaged in vacuum.

We then illustrated the use of this resonator in a sensing application by developing instruments for measuring its electrical properties and by including the unpackaged resonator in a scanning probe surface profiler setup. The interaction between the tuning fork and the surface under investigation influences the current through the tuning fork by perturbing the resonance frequency of the prong in contact with the

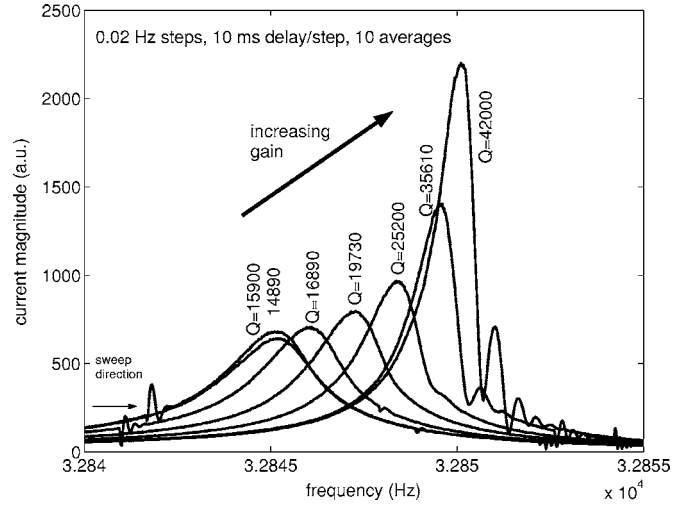


Fig. 9. Measurement of the quality factor enhancement of a tuning fork in air as a function of the feedback loop gain. Maximum enhancement is achieved when the circuit starts oscillating once the resonance frequency is reached during a sweep.

sample. The probe-sample distance is thus kept constant, leading to an accurate topography mapping, independent of other physical properties of the sample.

Finally, the quality factor was shown to be a tunable quantity which could be increased or decreased by injecting energy in phase or out of phase respectively with the input voltage. The oscillator is thus a limit condition of an infinite quality factor when the losses are compensated by the in-phase injection of energy.

ACKNOWLEDGMENTS

S. Ballandras (FEMTO-ST/LPMO, Besaçon, France) kindly provided access to the MODULEF-based (www-rocq.inria.fr/modulef/) finite element analysis software for modeling the tuning fork as shown in Fig. 2. The EDX analysis of the electrodes of a tuning fork was performed by L. A. Francis (IMEC, Leuven, Belgium).

^{a)}Electronic mail: jmfriedt@lpmo.edu

^{b)}Electronic mail: emile.carry@univ-fcomte.fr

¹Reference 547-6985 from Radiospares in France or from the manufacturer reference NC38LF-327 (www.foxonline.com/watchxtals.htm).

²M. P. Forrer, "A flexure-mode quartz for an electronic wrist-watch," in *Proceedings 23rd ASFC*, 157-162 (1969).

³H. Yoda, H. Ikeda, and Y. Yamabe, "Low power crystal oscillator for electronic wrist watch," in *Proceedings 26th ASFC*, 140-147 (1972).

⁴T. D. Rossing, D. A. Russel, and D. E. Brown, "On the acoustics of tuning forks," *Am. J. Phys.* **60**, 620-626 (1992).

⁵P. P. Ong, "Little known facts about the common tuning fork," *Phys. Educ.* **37**, 540-542 (2002).

⁶M. Soutif, "Vibrations, propagation, diffusion," Dunod Université, 196 (1982) (in French).

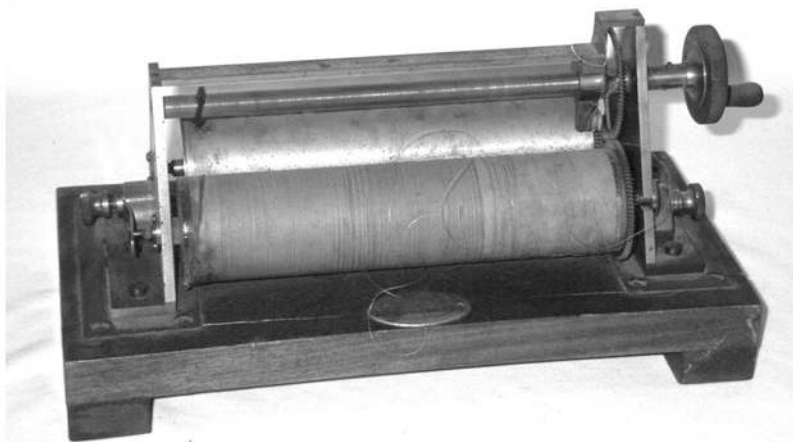
⁷L. Landau, and E. Lifchitz, *Theory of Elasticity* (Pergamon, New York, 1986) and (members.iinet.net.au/~fotoplot/acqf.htm).

⁸(www.ieee-uffc.org/freqcontrol/quartz/fc-conqz2.html).

⁹J. R. Vig and A. Ballato, "Frequency control devices," in *Ultrasonic Instruments and Devices*, edited by E. P. Papadakis (Academic, London, 1999), available at (www.ieee-uffc.org/freqcontrol/VigBallato/fcdevices.pdf). Also of interest is (www.ieee-uffc.org/freqcontrol/tutorials/vig2/tutorial2.ppt).

¹⁰K. Karrai and R. D. Grober, "Piezoelectric tip-sample distance control for near field optical microscopes," *Appl. Phys. Lett.* **66**, 1842-1844 (1995);

- (www2.nano.physik.uni-muenchen.de/~karrai/publications.html).
- ¹¹ K. S. Van Dyke, "The electric network equivalent of a piezoelectric resonator," *Phys. Rev.* **25**, 895 (1925).
 - ¹² D. W. Dye, "The piezo-electric quartz resonator and its equivalent electrical circuit," *Proc. Phys. Soc. London* **38**, 399–458 (1925), doi:10.1088/1478-7814/38/1/344
 - ¹³ The sum of the phase shifts of all elements in the loop, resonator + amplifier + phase shifter, must be a multiple of 2π , as mentioned in (www.rubiola.org/talks/leeson-effect-talk.pdf).
 - ¹⁴ (www.fairchildsemi.com/ds/CD/CD4060BC.pdf).
 - ¹⁵ C. Audoin and B. Guinot, *The Measurement of Time: Time, Frequency and the Atomic Clock* (Cambridge University Press, Cambridge, 2001), p. 86.
 - ¹⁶ J. W. G. Tyrrell, D. V. Sokolov, and H.-U. Danzebring, "Development of a scanning probe microscope compact sensor head featuring a diamond probe mounted on a quartz tuning fork," *Meas. Sci. Technol.* **14**, 2139–2143 (2003).
 - ¹⁷ "Selected papers on scanning probe microscopies," edited by Y. Martin, SPIE Milestone Series MS 107 (1994).
 - ¹⁸ F. J. Giessibl, "High-speed force sensor for force microscopy and profilometry utilizing a quartz tuning fork," *Appl. Phys. Lett.* **73**, 3956–3958 (1998).
 - ¹⁹ Y. Seo, W. Jhe, and C. S. Hwang, "Electrostatic force microscopy using a quartz tuning fork," *Appl. Phys. Lett.* **80**, 4324–4326 (2002).
 - ²⁰ M. Todorovic and S. Schultz, "Magnetic force microscopy using nonoptical piezoelectric quartz tuning fork detection design with application to magnetic recording studies," *J. Appl. Phys.* **83**, 6229–6231 (1998).
 - ²¹ D. W. Pohl, W. Denkt, and M. Lanz, "Optical stethoscopy: Image recording with resolution $\lambda/20$," *Appl. Phys. Lett.* **44**, 651–653 (1984).
 - ²² D. W. Pohl, U. C. Fischer, and U. T. Dürig, "Scanning near-field optical microscopy (SNOM)," *J. Microsc.* **152**, 853–861 (1988).
 - ²³ M. Todorovic and S. Schultz, "Miniature high-sensitivity quartz tuning fork alternating gradient magnetometry," *Appl. Phys. Lett.* **73**, 3595–3597 (1998).
 - ²⁴ J.-M. Friedt, "Realization of an optical profiler: Introduction to scanning probe microscopy," *Am. J. Phys.* **72**, 1118–1125 (2004).
 - ²⁵ J. W. P. Hsu, Q. Q. McDaniel, and H. D. Hallen, "A shear force feedback control system for near-field scanning optical microscopes without lock-in detection," *Rev. Sci. Instrum.* **68**, 3093–3095 (1997).
 - ²⁶ M. Stark and R. Guckenberger, "Fast low-cost phase detection setup for tapping-mode atomic force microscopy," *Rev. Sci. Instrum.* **70**, 3614–3619 (1999).
 - ²⁷ H. Edwards, L. Taylor, W. Duncan, and A. J. Melmed, "Fast, high-resolution atomic force microscopy using a quartz tuning fork as actuator and sensor," *J. Appl. Phys.* **82**, 980–984 (1997).
 - ²⁸ D. P. Tsai and Y. Y. Lu, "Tapping-mode tuning fork force sensing for near-field scanning optical microscopy," *Appl. Phys. Lett.* **73**, 2724–2726 (1998).



Wheatstone's Rheostat. Many modern electrical measurement techniques can be found in Charles Wheatstone's 1843 Bakerian Lecture, "An account of several new Instruments and Processes for determining the constants of a Voltaic Circuit." In his paper, Wheatstone makes use of the prefix *rheo*, from the Greek root meaning "to flow." A *rheostat* is a device for maintaining a constant current. To measure an unknown resistance, Wheatstone proposed that it be placed in series with a *rheoscope* (ammeter) and a *rheomotor* (source of EMF). The reading of the rheoscope was noted, and a rheostat inserted into the circuit in place of the unknown. The rheostat was adjusted to give the same current reading. The rheostat had previously been calibrated using Wheatstone's Bridge. The picture shows a Wheatstone-type rheostat by White of Glasgow in the collection of Miami University of Ohio. The near cylinder is made of wood with a shallow helical groove cut in it. As the cylinder is rotated, resistance wire unwinds from the wooden cylinder and winds up on the brass cylinder at the rear. (Photograph and Notes by Thomas B. Greenslade, Jr., Kenyon College).